

Dislocation-Mediated Conductivity in Oxides: Progress, Challenges, and Opportunities

Micah D. Armstrong, Kai-Wei Lan, Yiwen Guo, and Nicola H. Perry*



Cite This: *ACS Nano* 2021, 15, 9211–9221



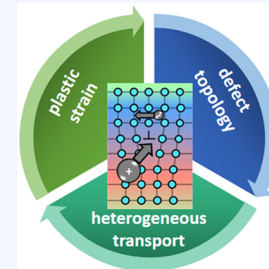
Read Online

ACCESS |

Metrics & More

Article Recommendations

ABSTRACT: Dislocations in ionic solids are topological extended defects that modulate composition, strain, and charge over multiple length scales. As such, they provide an extra degree of freedom to tailor ionic and electronic transport beyond limits inherent in bulk doping. Heterogeneity of transport paths as well as the ability to dynamically reconfigure structure and properties through multiple stimuli lend dislocations to particular potential applications including memory, switching, non-Ohmic electronics, capacitive charge storage, and single-atom catalysis. However, isolating, understanding, and predicting causes of modified transport behavior remain a challenge. In this Perspective, we first review existing reports of dislocation-modified transport behavior in oxides, as well as synthetic strategies and multiscale characterization routes to uncover processing–structure–property relationships. We outline a vision for future research, suggesting outstanding questions, tasks, and opportunities. Advances in this field will require highly interdisciplinary, convergent computational–experimental approaches, covering orders of magnitude in length scale, and spanning fields from microscopy and machine learning to electro-chemo-mechanics and point defect chemistry to transport-by-design and advanced manufacturing.



The ability of solid-state ionic materials, particularly air-stable complex oxides, to transport mass and charge selectively has long been leveraged and tailored to enable increasingly diverse applications, including electrochemical energy conversion/storage, sensors, optoelectronics, gas separation membranes, electrochromic windows, catalysts, memory elements, chemical actuators, and neuromorphic computing arrays. The point-defect chemical “bookkeeping”, summarized by Kröger and Vink and applied by Brouwer, has been a powerful framework for describing ionic and electronic charge-carrier concentrations and the impact of doping and gas atmosphere in the context of transport behavior.^{1,2} Recently, the interactions of these “zero-dimensional” point defects with nominally one- or two-dimensional (2D) extended defects have received increasing attention.³ Although there are ultimate limits on the extent to which charge carrier and point-defect populations can be tailored in the crystalline bulk by compositional means (e.g., solubility limits, accessible gas pressures, generation of compensating defects, defect association, Fermi level pinning), extended defects provide an extra degree of freedom for introducing novel transport and other functional behavior. Exotic effects that are not achievable in pristine bulk crystals can be realized through the disruption of regular crystallographic mass and charge periodicity at these extended defects. For example, the discoveries of anomalous enhancements in ionic conductivity at heterointerfaces in thin-film multilayers⁴ and ceramic composites,⁵ heightened electronic conductivity^{6,7} and ionic diffusivity^{8,9} at grain

Although there are ultimate limits on the extent to which charge carrier and point-defect populations can be tailored in the crystalline bulk by compositional means, extended defects provide an extra degree of freedom for introducing novel transport and other functional behavior.

boundaries, novel “mesoscopic” conductivity effects^{4,10} due to the dominance of interacting interfaces, 2D electron/hole gases at interfaces in oxide heterostructures,^{11,12} and tailororable ionic/electronic transference numbers via varied interface density^{13,14} have not only established the field of “nanionics,”¹⁵ but also provided possibilities for novel materials design strategies, devices, and performance.

Published: May 27, 2021



A number of structural and chemical factors, spanning many length scales, may contribute to distinct local and macroscopic transport behavior. The core of an extended defect (length

A number of structural and chemical factors, spanning many length scales, may contribute to distinct local and macroscopic transport behavior.

scale: angstroms) can be a region of modified atomic spacing, coordination, and stoichiometry,¹⁶ with implications for altered concentrations¹⁷ and mobilities of intrinsic ionic and electronic species or extrinsically doped/intercalated ions. Further, in ionically bonded solids, extended defects can be charged at their core, giving rise to adjacent space-charge regions (length scale: nanometers to tens of nanometers) comprising accumulation of mobile carriers of the opposite charge or depletion of mobile carriers of the same charge.¹⁸ The extent and character of these space-charge profiles depend on the doping or impurity levels and thermal and electrical history,¹³ among other factors. In addition, inhomogeneous strain fields (length scale: nanometers) can surround dislocations, resulting in locally varying defect formation energies and mobilities, as well as a possibility for local defect association and dopant segregation.^{19,20} At sufficient concentrations, extended defects may interact through overlapping space-charge regions or strain fields or intersecting cores, creating “mesoscopic” transport properties^{4,10} or the possibility for percolation behavior (length scale: micrometers to millimeters). Local transport is expected to be anisotropic, with different barriers along (parallel to) *versus* across (perpendicular to) extended defects with high aspect ratios. Depending on the processing route, the microscale structure of extended defect networks can be highly diverse in terms of core structure, concentration/volumetric density, and homogeneity of location in the material sample.²¹ Beyond these static considerations, the multiscale structure and properties of extended defects and their arrays may be dynamic and heterogeneously sensitive to gas atmosphere, thermal conditions, electrical field, doping levels, exposure to light, and mechanical stress during processing and operation. Systemati-

cally separating and understanding each individual structural and chemical contribution to behavior, as well as their interactions, remain central challenges for this field (Figure 1).²¹

In this Perspective, we focus specifically on the emerging topic of dislocation-induced transport modifications in oxides, first summarizing the current state-of-the-art of (a) synthetic strategies for tailoring dislocation nano- and mesostructures, (b) approaches for characterizing multiscale dislocation structure–transport property relationships, and (c) reported modifications to ionic and electronic conductivity. We also highlight challenges, open questions, and opportunities, which can drive future research. These forward-looking considerations include applications of synthetic routes, characterization methods, simulations, design, and advanced manufacturing. They revolve around several cross-cutting needs for (i) descriptors that enable rapid prediction and classification of dislocation core structure, charge, and space charge profiles, (ii) multiscale *in situ* characterization that expands to cover a broader range of compositions, and (iii) models of macroscopic transport behavior that bridge these length scales to incorporate dislocation heterogeneity, anisotropy, mesoscale interactions, and dynamic behavior.

FORMING DISLOCATIONS: SYNTHETIC STRATEGIES

Dislocations can be generated by different routes, including the joining of misaligned single crystal surfaces to form a bicrystal interface, the growth of thin films with moderate lattice mismatch to the underlying substrate, and the postprocessing application of macroscopic or focused mechanical stress (Figure 2). Correspondingly, the types of dislocations and their arrangement and distribution at micro- or mesoscopic scales vary with processing routes. Periodically arranged

The types of dislocations and their arrangement and distribution at micro- or mesoscopic scales vary with processing routes.

networks of dislocations can be introduced in a bicrystal with a controlled crystallographic relationship between the

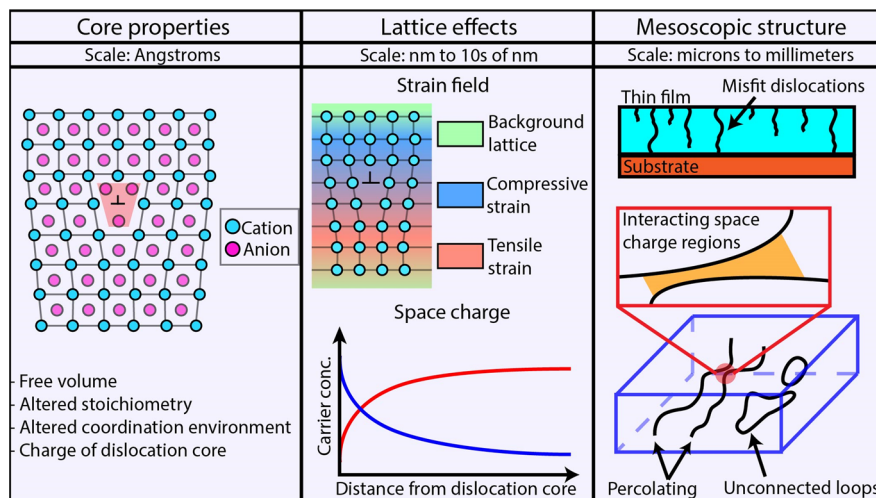


Figure 1. Multiscale structural and chemical contributions to modified transport behavior at dislocations.

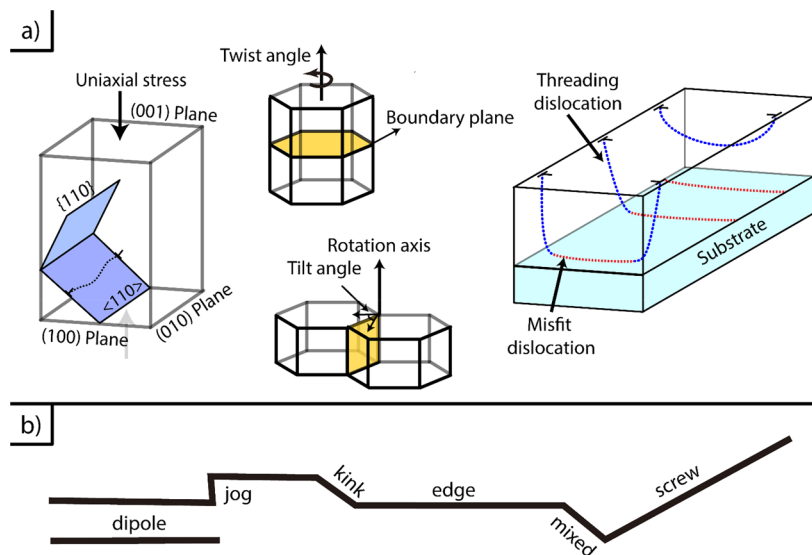


Figure 2. (a) Selected methods of forming dislocations in single crystals, bicrystals, and thin films/heterointerfaces, along with their structures. (b) Possible components of dislocation character, depending on processing (based on graphical concepts in ref 21).

constituent two crystals, and regular dislocation arrays are also formed at low-angle grain boundaries. In general, depending on the degree of misorientation, low-angle tilt grain boundaries consist of edge dislocations, while low-angle twist grain boundaries consist of screw dislocations.²² More complex mesoscopic dislocation structures can be generated by high misorientation angles due to extended defect overlap. Distances between dislocations in low-angle tilt grain boundaries can be predicted by Frank's equation, where the spacing is inversely proportional to the tilt angle of the boundary.²² A similar relationship exists to predict average dislocation spacing on the basis of lattice mismatch at a heterointerface given the length of the appropriate Burgers' vector component (spacing is inversely proportional to mismatch).²³ Pulsed laser deposition (PLD), molecular beam epitaxy (MBE), and atomic layer deposition (ALD) are appropriate techniques to synthesize oxide thin films with high interface quality.²⁴ During the growth process, dislocation half-loops initiate at the surface of the film, and they become larger and propagate to reach the substrate/film interface as the film thickness increases. Thus, misfit dislocations are formed along the interface to accommodate the high elastic strain energy imposed by the substrate–film lattice parameter mismatch, and threading dislocations form across the thin film and bend at the interface into misfit dislocations.²⁵

Postsynthesis, dislocations can be introduced through the application of mechanical stress, leading to a wide variety of nonuniform mesoscale dislocation structures (*e.g.*, hierarchical tree-like arrangements).²⁶ Bulk plastic deformation provides a maximized dislocation density compared with polishing; local stress can also be induced through other methods, such as nanoindentation. Uniaxial stresses are often applied in the research context because well-defined critical resolved shear stresses (CRSS) on an individual slip system may be obtained.²⁷ Most ceramics are deformed at high temperature, although some ceramics can be deformed at room temperature. For example, a simulation performed by Hirlé *et al.* showed that dislocations glide easily in strontium titanate (SrTiO_3) at low temperature, and the ends of edge dislocations serve as pinning points that greatly reduce the mobility of the

dislocations as temperature increases.²⁸ In addition, small loops, extensive dipoles, and dislocation lines with mixed character including kinks and jogs have been obtained in uniaxially stressed SrTiO_3 single crystals.²¹ Conversely, deformation is controlled by high lattice friction in magnesium oxide (MgO) at room temperature, which is an indication of a Peierls mechanism, and MgO may have straight and long screw dislocations gliding at lower velocity compared to edge dislocations.²⁷ Therefore, the activated slip system generating dislocations is highly dependent on temperature and material. Further, strain rate plays a significant role in the dislocation–defect interactions and structure developed.²⁹ As a result, the complexity of mesoscopic structures and temperature-dependent slip systems complicates the understanding of the effect of dislocations on functional ceramics.

MULTISCALE CHARACTERIZATION METHODS

Various characterization techniques and methods are used to study the atomic and mesoscale structure, chemistry, and transport behaviors of dislocations.

Structure and Chemistry. Transmission electron microscopy (TEM) and scanning transmission electron microscopy (STEM) can provide direct images of dislocations. Such images indicate the presence, distribution, position, direction, density, and even motion of dislocations clearly and can enable determination of the Burgers vectors.^{30,31} High-angle annular dark-field (HAADF) and annular bright-field (ABF) techniques are used frequently when dislocations are observed. For example, Spurgeon *et al.* used inverse, masked fast Fourier transform (IFFT) with STEM-ABF imaging to help better present the existence of misfit dislocations.³² By atomic-resolution electron energy loss spectroscopy (EELS) and energy dispersive X-ray spectroscopy (EDS) imaging, the distribution of some elements can be observed in HAADF-STEM images.³³ Similarly, to understand the ionic conductivity at edge dislocations, researchers have used HAADF-STEM combined with EDS at atomic resolution to quantify the strain locally; Feng *et al.* applied geometric phase analysis (GPA) in order to obtain the strain field around the dislocation core.³⁴ Field ion microscopy (FIM) and atom

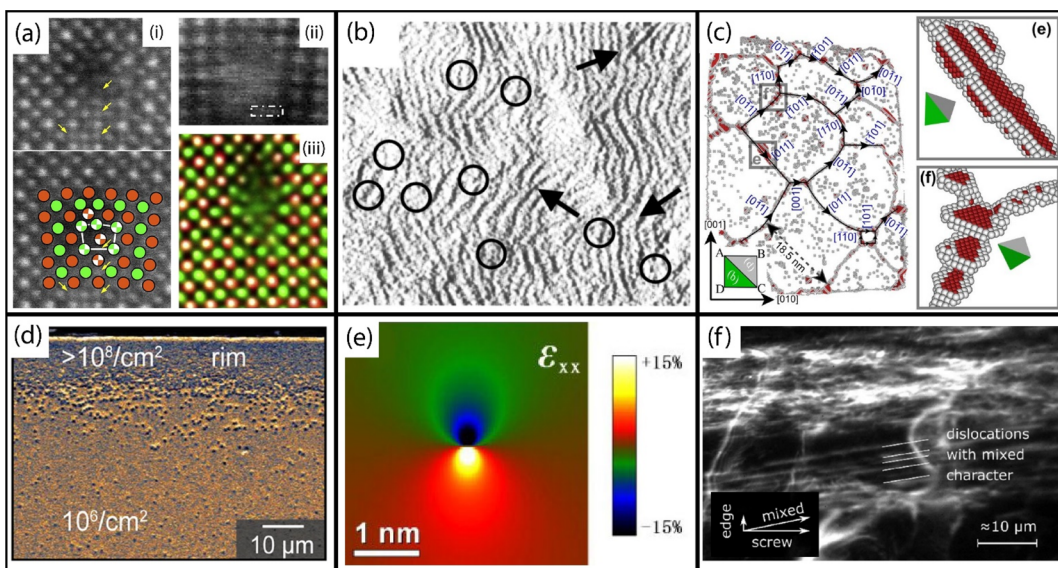


Figure 3. Selected methods for elucidating structure–property relationships pertaining to dislocations: (a) High-angle annular dark-field scanning transmission electron microscopy, (b) conductive atomic force microscopy, (c) atom probe tomography, (d) scanning electron microscopy, (e) strain field mapping, and (f) dark-field X-ray microscopy. Panel a reprinted with permission from ref 33. Copyright 2015 Elsevier. Panel b reprinted with permission from ref 40. Copyright 2002 AIP Publishing. Panel c reprinted with permission from ref 42. Copyright 2015 Elsevier. Panel d reprinted with permission from ref 35. Copyright 2019 Rodenbacher *et al.* Panel e Reprinted with permission from ref 41. Copyright 2008 Elsevier. Panel f reprinted from ref 21. Copyright 2020 American Chemical Society.

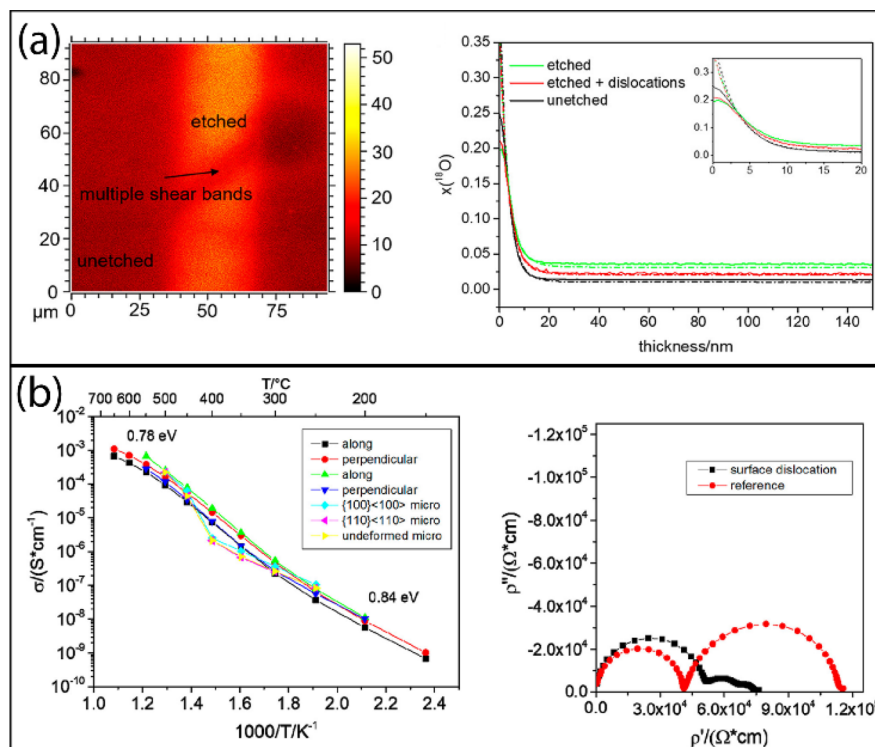


Figure 4. Selected methods for analyzing the transport properties of ionic solids: (a) tracer diffusion/secondary ion mass spectrometry and (b) ac impedance spectroscopy. Reprinted from ref 21. Copyright 2020 American Chemical Society.

probe tomography (APT) can also provide high resolution observation of dislocations. Indirectly and at lower resolution, scanning electron microscopy (SEM) can be used to observe the dislocation structures. If the dislocation lines in the material intersect with the surface of the material, the chemical stability near the intersection point will be lower than other parts of the surface due to the existence of the dislocation

stress field. Therefore, after an etching step with a HF solution, the position of dislocations can be observed as etch pits on the surface.³⁵ Dark-field X-ray microscopy (DFXM) has also been applied.²¹ Selected examples of results from these techniques are shown in Figure 3.

Simulation methods complement these experimental approaches. Atomistic models can be set up using density

functional theory (DFT) or DFT+U in a periodically repeating supercell with a dislocation dipole (screw dislocation) or a slab with an extra half-plane of atoms (edge dislocation).^{19,31} Molecular dynamics (MD) simulations have been used to show the vacancy structure along a screw dislocation in MgO.³¹ The hybrid Monte Carlo and molecular dynamics approach (MCMD) has been applied to show the effect of dislocations on the charged defects' local distribution and ionic diffusion in CeO₂.¹⁹ The concurrent atomistic-continuum (CAC) method also works well in simulating the dynamics of dislocation nucleation and migration in SrTiO₃, albeit with slightly lower accuracy than corresponding fully atomistic MD simulations, due to reduction in the degrees of freedom.³⁶

Transport. The tracer diffusion method can be used in the studies of atomic transport in ionic solids. Fast diffusion along dislocations can lead to depth concentration profiles exhibiting two characteristic regions, with the lower concentration "tail" providing insight into transport along dislocations.³⁷ Radio-isotopes for diffusion studies are available for most elements, but some common mobile ions do not require radioactive tracers, including Li, F, and O; stable ¹⁸O and ⁶Li isotopes exist, and Li and F can also be studied through nuclear magnetic resonance (NMR) methods.³⁸ Time-of-flight secondary ion mass spectrometry (ToF-SIMS) analysis after ¹⁸O tracer diffusion has been growing in spatial resolution and can clearly indicate laterally inhomogeneous oxygen depth profiles in different regions of the sample.²¹ Both dc and ac electrical measurements (e.g., *versus* oxygen partial pressure, temperature, or dc bias) provide further insight into both electronic and ionic transport behavior. At sufficient density, dislocations can impact the pO₂-dependence of conductivity through modifying carrier concentrations, and transport across extended defects often exhibits non-Ohmic behavior due to carrier accumulation or depletion regions. AC impedance spectroscopy enables separation of bulk and extended defect transport responses indirectly in many cases, and with temperature-dependent studies, one may observe differences in local activation energies.³⁹ Direct local measurements are also possible with conductive atomic force microscopy (c-AFM) techniques.⁴⁰ Selected examples of dislocation transport studies are shown in Figure 4.

EFFECTS OF DISLOCATIONS ON TRANSPORT

Research into the effect of dislocations on ionic transport properties began in earnest in the mid-2000s with experiments analyzing the effect of dislocations on the ionic conductivity of yttria-stabilized zirconia (YSZ).^{43,44} In two studies by Otsuka *et al.*, the ionic conductivity was shown to increase with the introduction of dislocations, but the issue of the "healing" of the dislocations at high temperatures was discussed.^{43,44} The latter of these early studies also showed that the ionic conductivity in this system increased when dislocations were present regardless of crystallographic orientation.⁴⁴ Although the early work regarding YSZ largely reported positive effects, some going as far as to present superionic conductivity as a result of added dislocations,⁴⁵ some of this work failed to isolate the contribution of dislocations from other potential causes of modified transport behavior.⁴⁶ Reports of colossal increases in conductivity of majority ionic carriers *via* extended defects should be treated carefully, given the other contributors to measured resistance that may be present (e.g., electronic conductivity, surface proton conductivity, or hetero-interface effects in thin films including intermixing, "polar catastrophe"/

electrostatic gating, and elastic strain). Recent studies have presented possible mechanisms for improved ionic transport in YSZ due to dislocations, including pipe diffusion along dislocation cores,³⁴ which has, however, been discounted in other work.⁴⁷ For example, studies done by Korte *et al.* and Schichtel *et al.* also found increases in conductivity with respect to extended defect concentration, but the increase was attributed to the strain fields around the dislocations rather than to pipe diffusion.^{23,48,49} The lack of alignment in the produced dislocations, which has been confirmed for both misfit dislocations⁴⁷ and mechanically induced dislocations,⁴⁶ was proposed as one argument against pipe diffusion in each case.

After the early findings with YSZ, researchers began to study these dislocation-modified transport properties in a limited selection of additional compositions. For example, rutile-structured TiO₂ was chosen due to the low solubility of dopants, which necessitates the use of higher order defects to tailor transport properties.^{39,50} Two studies by Adepalu *et al.* on TiO₂ determined the effect of mechanically created dislocations on the ionic and electronic conductivity.^{39,50} In the single crystal case, increases in positive carrier (p-type electronic, ionic) conductivity were observed parallel to the dislocations and attributed to space charge effects surrounding the negatively charged dislocation core.³⁹ In the polycrystalline case, the addition of dislocations caused a shift from predominantly electronic to ionic conductivity, which the authors attributed to increased oxygen vacancy and titanium interstitial (Ti_i⁺ and v_O⁻) concentrations in the space charge regions around the dislocations, a phenomenon not feasible through chemical doping alone.⁵⁰

Recent work has focused primarily on SrTiO₃ (STO), a prototypical model perovskite with mixed ionic-electronic conduction and an array of possible applications, such as fuel cell electrodes and catalysis, upon doping.⁵¹ Many of these studies demonstrate the detrimental effects of the positively charged dislocation core in STO, which serves to block, rather than to enhance, oxygen ion conduction (*via* the positively charged oxygen vacancy mechanism).^{21,51,52} These works address this phenomenon in the bulk material⁵¹ and surface region.⁵² Although depression of oxygen ion conductivity inhibits use in many applications, Rodenbacher *et al.* demonstrated that dislocations can serve as electron channels given their propensity to reduce preferentially upon voltage application, which may be beneficial in optimizing materials such as STO for memristive applications.³⁵ A prominent feature of the literature on STO is that the agreement between simulation and experimental work demonstrates repeatability and provides confidence in the results.

Although less numerous, similar studies have been conducted to determine the effects of dislocations on ionic transport in BaZrO₃ (BZO).^{53–55} For BZO, two experimental studies, both on BZO thin-films on NdGaO₃ substrates, showed significant increases in proton conductivity as a result of misfit dislocations that form due to the lattice mismatch between BZO and NdGaO₃.^{53,54} Although the authors found similar results, the explanations they proposed are different. Felici *et al.* determined that the effect was due to the incorporation of hydroxyl groups at dislocations, which required protons to be integrated to provide charge balance, whereas Liu *et al.* proposed that the increase in both barium and oxygen vacancies could have enabled the higher conductivity.^{53,54} For oxygen diffusion in these systems,

Table 1. Summary of Existing Work Measuring or Simulating the Effect of Dislocations on Transport Properties in Oxides

material	type of sample	substrate	method of forming dislocations	effect on transport	explanation	year	ref
YSZ	single crystal		mechanical stress	~9% increase in electrical conductivity	pipe diffusion	2003	43
	single crystal		mechanical stress	~5–15% increase in ionic conductivity	increased oxide ion mobility along dislocation lines	2004	44
	thin film	Sc ₂ O ₃	lattice mismatch	increase in conductivity with an increase in the degree of mismatch between the substrate and film	effects in low mismatch systems: strain fields	2009	56
	multilayers	Lu ₂ O ₃			effects in high mismatch systems: dislocation density and atomic arrangement		
Al ₂ O ₃	Al ₂ O ₃	Sc ₂ O ₃	lattice mismatch	increase in conductivity with an increase in the degree of mismatch between the substrate and film	increase in ionic conductivity is likely due to strain effects that arise from lattice mismatch	2009	48
thin film multilayers	Y ₂ O ₃	Sc ₂ O ₃	lattice mismatch	decrease in ionic conductivity of the YSZ phase was measured with increasing interfacial density	decrease in transport was attributed to compressive strain fields around the YSZ/Sc ₂ O ₃ interface (not dislocations)	2010	49
thin film multilayers	Sc ₂ O ₃	MgO or SrTiO ₃	lattice mismatch	3.5 orders of magnitude increase in ionic conductivity	dislocation lines act as fast transport paths	2010	45
thin film	SiO ₂	peening		conductivity decreases as a result of peening and recovers after annealing	dislocation lines will often not be parallel to the direction of transport	2015	46
thin film	MgO	Al ₂ O ₃	lattice mismatch	no enhancement in conductivity was found; interfaces were found to be more resistive	strain effects were minimal, no transport along dislocations was found, and grain boundaries resulted in the higher resistivity of the interface	2017	47
		LaAlO ₃					
		NdGaO ₃	bicrystal method	up to 3 orders of magnitude increase in ionic conductivity	pipe diffusion	2019	34
	bicrystal thin film	MgO	lattice mismatch	significant increase in conductance with respect to film thickness	space charge effects and oxygen vacancies at the interface	2017	30
STO	single crystal		mechanical stress	n-type conductivity increases by 50× at extremely low pO ₂	overlapping space charge regions	2017	51
	single crystal		polishing	p-type conductivity decreases by 50× at higher pO ₂	space charge	2018	52
	single crystal		polishing	decrease in oxide ion diffusivity	filamentary conduction along dislocations under reducing conditions	2019	35
	single crystal		mechanical stress	n-type conductivity increases by a factor of 10 ⁴ in the vicinity of dislocations	mesoscopic structure, core structure, and space charge	2020	21
	bicrystal		bicrystal method	dependent on mesoscopic structure of defects	filamentary conduction along dislocations under reducing conditions	2020	57
	single crystal		mechanical stress	increased n-type conductivity along dislocations at high pO ₂ , p-type conduction and ionic conduction are greatly enhanced	space charge	2013	39
				at low pO ₂ , there is no change in n-type conductivity	negative dislocation cores, space charge regions		
				ionic conductivity becomes the dominant conduction mechanism			
Pellet			spark plasma sintering	diffusion along dislocations up to 3× faster than in bulk	negative dislocation cores, space charge regions	2014	50
			lattice mismatch				
La _{0.8} Sr _{0.2} MnO ₃	thin film	LaAlO ₃ or SrTiO ₃			diffusion along dislocations, mesoscopic structure	2017	25
MgO	simulation					2010	58
Y-doped BZO	thin film	NdGaO ₃	lattice mismatch	significant reductions in activation energy for diffusion; significant increases in diffusivity are predicted	pipe diffusion	2019	54
BZO	simulation	NdGaO ₃	lattice mismatch	significant increase in proton conduction	charge balance due to the localization of hydroxyl groups along dislocations	2019	55
CeO ₂	simulation			significant increase in oxide ion conduction	pipe diffusion	2019	53
				significant increase in protonic conduction in films <20 nm thick	space charge, accumulation of cation and anion vacancies		
				up to 1.5× increase in diffusivity of oxide ions	strain effects	2015	19

simulations by Li *et al.* propose pipe diffusion as the mechanism, so the explanations for dislocation-modified transport can vary greatly based on the study, carrier in question, processing route, including impurity incorporation (if experimental), and types of dislocations present.⁵⁵ For a simplified summary of reported effects of dislocations on transport in oxides, where diffusivity or conductivity was directly measured or simulated, refer to Table 1.

OPPORTUNITIES, QUESTIONS, AND CHALLENGES

Significant computational and experimental research opportunities exist broadly in the area of understanding and classifying dislocation structure–transport–property relationships across multiple length scales and compositions and in applying these insights in advanced manufacturing strategies toward transport-by-design. Fundamental considerations in-

Significant computational and experimental research opportunities exist broadly in the area of understanding and classifying dislocation structure–transport property relationships across multiple length scales and compositions and in applying these insights in advanced manufacturing strategies toward transport-by-design.

clude the following: What unique transport benefits are conferred *via* dislocations that are not accessible by potentially easier means such as doping or elastic strain? What might be the theoretical bounds on tailoring macroscopic conductivity through dislocations? What level of inter-dislocation variation among core structures, charges, local transport properties, and extent of conductivity anisotropy exists for a given composition or processing route? Which chemical features (e.g., dopant or impurity size or charge mismatch *versus* host site, defect formation enthalpies, defect mobilities) are most significant for determining the core charge under equilibrium or under kinetically limited process conditions? How common is fast pipe diffusion along dislocation cores in oxides, and is this enhancement only possible for extrinsic or minority charge carriers (or, are fast bulk ion conductors affected adversely and poor bulk ion conductors affected beneficially)? Applied considerations include the following: How stable are dislocation structures and chemistries under operating conditions of applied field, stress, gas atmosphere, or temperature, and can dynamic dislocation behavior be leveraged in applications, for example, for switching or memory? Which manufacturing tools can enable direct writing of well-defined dislocation structures or high-throughput synthesis of ordered and aligned dislocation arrays? Which applications of complex oxides might benefit from precise dislocation structures where these have not yet been tested? In the following paragraphs, ten areas of outstanding research tasks and challenges are enumerated.

1. Leverage Advanced Characterization Tools to Understand the Structure of Buried Dislocations and their Three-Dimensional Arrays across Multiple Length Scales Spanning Orders of Magnitude. There is a particular need to identify the atomic-scale structure and

composition of dislocation cores for different kinds of dislocations, processing routes, and compositions. Even for one of the most-studied compositions, SrTiO₃ (a prototypical perovskite), only limited types of dislocation core structures have been observed experimentally, for example, within the {110} {110} and {110} {110} slip systems.^{21,33} Dislocations produced at a boundary of a bicrystal *versus* those generated mechanically in a single crystal *versus* those grown in thin films can exhibit very different characters even if they are in the same slip system.²¹ To characterize these dislocations, HAADF-STEM with EELS/EDS and strain mapping is particularly appropriate.³³ Similarly, advanced high-resolution tomographic methods (electron tomography,⁵⁹ atom probe tomography⁶⁰) may be of use, not only for observing 3D array architectures and interactions among dislocations but also for characterizing differences among individual dislocation structures and chemistries down to atomic resolution.

2. Quantify Transport Anisotropy and Variability among Dislocation Structures for a Given Composition.

One limitation of traditional atomic resolution microscopy is the uncertainty over whether individually observed extended defects are representative; therefore, methods that assess ensembles of extended defects over wider length scales yet with adequate resolution to characterize individual dislocations and to quantify their structural and chemical diversity statistically are highly valuable. Similarly, assessments of variability of transport parameters, including local conductivity, electrical width, core charge, and activation energy, can complement such structural and chemical studies. A combination of ac and dc electrical measurements, SIMS, and EBSD imaging has recently been applied to observe variability in grain boundaries of CeO₂ bicrystal fibers and has provided insight into the chemical origin of the variability in core charge.⁶¹ Similarly, Xu *et al.* combined atom probe tomography with electron holography to provide insight into the diversity of space charge potentials among grain boundaries in polycrystalline (Ce,Sm)O₂.⁶² Analysis of transport anisotropy can be performed by creating ordered arrays of aligned dislocations and performing macroscopic transport measurements parallel and perpendicular to the alignment direction.²¹ Local studies along and across individual dislocations with microelectrodes or conductive AFM²⁶ may also be possible. Sometimes frequency-dependent impedance measurements enable separation of the bulk and dislocation contributions to conductivity on the basis of their different time constants, primarily when extended defects are blocking.⁶³

3. Bridge Local and Macroscopic Transport Behavior of Dislocations Considering Interdislocation Heterogeneity, Interactions, and Mesoscale Structure.

Composite and effective medium models⁶⁴ may be applied to model macroscopic transport behavior considering the dislocations as one phase and the bulk as the other phase, as has been applied with some success to the case of grain boundary transport in polycrystalline ceramics.^{13,65,66} As with grain boundaries, the models may be tailored to account for locally anisotropic transport in the extended defects, for shape effects (perhaps considering bulk regions bounded by dislocation arrays as “grains”), and for volume fraction of the extended defect “phase”.⁶⁵ Nonetheless, biphasic composite models may fail to account adequately for (a) interdefect variability and (b) intradefect inhomogeneity inherent in space charge-type concentration profiles or inhomogeneous dopant/impurity segregation and (c) irregular (nonperiodic) or hierarchical

arrays of dislocations. Pixel-based finite difference modeling may be of benefit in these more complex cases.

4. Assess Validity and Limits of Existing Models (e.g., Space Charge Models) Used to Explain Local Transport Behavior. Space-charge regions adjacent to charged dislocations have been invoked to explain modified macroscopic conductivity at a qualitative level in dislocation-rich TiO_2 and SrTiO_3 ^{39,51} and its oxygen partial pressure dependence. However, commonly used space charge models, such as Mott–Schottky and Gouy–Chapman solutions of the Poisson–Boltzmann equation, were developed for dilute situations and may not be appropriate for the heavily doped and solid-solution compositions more common in applications. For example, cation rearrangement and nonstoichiometry at $(\text{La},\text{Sr})\text{MnO}_{3\pm\delta}$ extended defects¹⁶ are not predicted by simple space charge models. A recent Poisson–Cahn⁶⁷ approach may be more beneficial for nondilute cases, but more widespread quantitative comparison of local chemistry and transport behavior to model predictions should be pursued for a variety of compositions. Existing models do not incorporate chemo-mechanical effects, and given heterogeneous strain fields around dislocation cores, they may not fully account for transport behavior until they are modified to include the interplay of chemical stress, mobility, and stoichiometry.

5. Expand the Range of Compositions Treated, Including Nondilute Systems. With the exceptions of YSZ, LSM, and BZY, most compositions treated to date are nominally undoped. In practical applications, including those listed in the introduction, higher doping levels or solid solutions tend to be more common. Further, the types of charge carriers in these studies have been limited (see Table 1). Studies of additional inorganic cation conductors and mixed cation–electronic conductors may be of particular interest for electrochemical energy storage applications, although space charge effects may be suppressed in systems with high dopant and carrier concentrations. Further studies of intercalated *versus* intrinsic ion transport could be pursued. In addition to dopant concentration, one may also consider nondilute dislocation concentrations. In existing studies, often dislocations have not been sufficiently proximal to induce overlap of any space-charge regions and mesoscopic behavior.

6. Advance High-Throughput Simulation Capabilities for Predicting Dislocation Core Structure and Charge. Accurate simulations of core stoichiometry, charge distribution, dopant segregation, and strain fields may be too computationally expensive to apply to screen many types of stable dislocation structures across many host compositions and mobile carrier types. However, rapid screening would be beneficial to build a larger framework and classification system of structure–property relationships with predictive power. Are there computationally cheap methods for predicting at least the sign of the core charge across various compositions and dislocation types, for example, using descriptor proxies such as vacancy formation enthalpies or other classification schemes?

7. Assess the Likely Bounds on the Magnitude of Modified Transport Effects Expected and Whether Dislocations Can Surpass Benefits of Other Means of Modifying Transport. It is an open question whether dislocations can further enhance conductivity of the majority charge carrier in a material that is already nearly optimized in the bulk through doping. Elastic strain, which exists locally around the dislocation core, is known to modify transport, increasing conductivity in tension and decreasing it in

It is an open question whether dislocations can further enhance conductivity of the majority charge carrier in a material that is already nearly optimized in the bulk through doping.

compression,^{49,68–70} but multiple strain states can exist around dislocations, and strain interacts with electrostatic effects and redistribution of mobile species. Some early simulations and measurements are not encouraging from the perspective of majority ionic species transport.^{39,46,47,49–51} Do dislocations only benefit transport of minority or extrinsic carriers, or only help majority carrier transport in systems that are not optimized in the bulk? Further realistic simulations and measurements of the magnitude by which dislocations can modify transport are needed, particularly covering a variety of charge-carrier types. Note that one benefit of dislocations compared to doping or elastic strain is the heterogeneity of transport pathways, given the high aspect ratio of the extended defects; for example, preferential electroreduction along dislocations has been reported,^{35,71} so they can act as conductive nanowires embedded in a less conductive matrix. A further benefit may be the dynamic nature of dislocation local structure and mesostructure (upon application of temperature,⁴³ electric field,³⁵ stress,²⁹ etc.) and the ability to modify transport behavior *in situ* in a nonvolatile manner. Both of these attributes may be beneficial in the context of memory or switching devices⁷¹ for providing means to repeatable and reconfigurable transport behavior. Inhomogeneous transport (including non-Ohmic behavior), polarization, and surface chemistry attributed to dislocations have also been leveraged in applications including varistors,⁷² barrier layer capacitors,⁷³ and catalysts.⁷⁴

8. Create a Taxonomy of Dislocation Structure–Transport–Property Relationships and Integrate It into a Larger Classification Scheme of Extended Functional Defects. This goal is to identify structural or chemical features that correlate with core charge or transport behavior and serve as a means of classifying dislocation types in the context of transport. Such a classification scheme could be predictive of behavior for untested compositions or dislocation structures. Machine learning⁷⁵ could be an appropriate tool for identifying underlying structure–property relationships or means of grouping results, although there are sparse data at present; high-throughput simulations may assist. More broadly, classification of dislocation transport behavior within a wider framework of extended defects may be possible; for example, certain grain boundaries and semicoherent heterointerfaces are described as planar dislocation arrays.

9. Advance Dynamic Dislocation Studies and Assessments of Long-Term Stability. Further characterization of time-dependent dislocation core and mesoscale structure, perhaps with protocols for accelerated testing, will help to identify suitable operational conditions and compositions from the standpoint of stability as well as kinetics and mechanisms of instability. Additional simultaneous *in situ* studies of charged dislocation dynamics and corresponding local properties under driven conditions (e.g., electrical fields, light, or plastic deformation) can also be pursued, for relevance to the selection of device operation conditions, potential to induce switching behavior or write nonbinary transport states, and

identification of transient or metastable emergent defect structure–property correlations.

10. Develop Advanced Nanomanufacturing of Dislocations-by-Design, Considering All the Relevant Length Scales.

The ability to synthesize dislocation arrays with tailored spacing, orientation, dislocation type, and even atomic-scale core structure would be foundational to advanced manufacturing of tailored transport behavior. Integration of nanoindentation⁷⁶ for direct writing, film growth strategies with atomic-scale control, or alternative well-defined stress application methods for periodic or ordered arrays with high-throughput processing could be of interest. For example, ordered arrays of misfit dislocations can form for intermediate lattice parameter mismatches between substrate and film, with the degree of mismatch influencing the spacing between dislocations.⁷⁷ Such arrays can generate periodic strain and surface patterns that modulate transport at the ~20 nm scale.⁷⁸

CONCLUSIONS AND OUTLOOK

The extra degree of structural and chemical freedom provided by dislocations in ionic systems provides a promising route to modify charge and mass transport beyond conventional limits of equilibrium bulk doping. Because studies of dislocation–transport relationships have covered only limited compositions and mesoscale architectures, significant opportunities for both fundamental and applied research exist. These studies must span and integrate information across orders of magnitude in length scale. They are also inherently interdisciplinary, calling for expertise in manufacturing, mechanics, microscopy, defects and transport, atomistic simulations, continuum modeling, and device testing—all under realistic operating conditions. Although the ultimate extent to which dislocations can be leveraged to tailor ionic and electronic transport has not yet been fully tested, there is hope in the dramatic effects previously reported for other kinds of extended defects in the broader nano-ionics field and in the unique benefits of heterogeneous and potentially reconfigurable transport architecture enabled by dislocations. A concerted, collaborative effort to develop structure–property relationships and extended defect taxonomy, coupled with high-throughput simulation and nanomanufacturing, may pave a new route to transport-by-design.

AUTHOR INFORMATION

Corresponding Author

Nicola H. Perry – Department of Materials Science & Engineering and Materials Research Laboratory, University of Illinois at Urbana–Champaign, Urbana, Illinois 61801, United States;  orcid.org/0000-0002-7207-2113; Email: nhperry@illinois.edu

Authors

Micah D. Armstrong – Department of Materials Science & Engineering and Materials Research Laboratory, University of Illinois at Urbana–Champaign, Urbana, Illinois 61801, United States

Kai-Wei Lan – Department of Materials Science & Engineering and Materials Research Laboratory, University of Illinois at Urbana–Champaign, Urbana, Illinois 61801, United States

Yiwen Guo – Department of Materials Science & Engineering and Materials Research Laboratory, University of Illinois at Urbana–Champaign, Urbana, Illinois 61801, United States

Complete contact information is available at: <https://pubs.acs.org/10.1021/acsnano.1c01557>

Notes

The authors declare no competing financial interest.

ACKNOWLEDGMENTS

The authors acknowledge the National Science Foundation Grant No. 2037898 (NSF-CMMI Future Manufacturing) and Grant No. 1922758 (DIGI-MAT PhD Traineeship, NSF-DGE) for research and education related to the topic of this Perspective. Any opinions, findings, and conclusions or recommendations expressed in this material are those of the authors and do not necessarily reflect the views of the National Science Foundation.

REFERENCES

- (1) Kröger, F. A.; Vink, H. J. Relations between the Concentrations of Imperfections in Crystalline Solids. In *Solid State Physics*; Seitz, F., Turnbull, D., Eds.; Academic Press: 1956; Vol. 3, pp 307–435.
- (2) Brouwer, G. A General Asymptotic Solution of Reaction Equations Common in Solid State Chemistry. *Philips Research Reports* 9, 1954.
- (3) Perry, N. H.; Harrington, G. F.; Tuller, H. L. Electrochemical Ionic Interfaces. In *Metal Oxide-Based Thin Film Structures*; Pryds, N., Esposito, V., Eds. Elsevier: 2018; Chapter 4, pp 79–106.
- (4) Sata, N.; Eberman, K.; Eberl, K.; Maier, J. Mesoscopic Fast Ion Conduction in Nanometre-Scale Planar Heterostructures. *Nature* 2000, 408, 946–949.
- (5) Liang, C. C. Conduction Characteristics of the Lithium Iodide-Aluminum Oxide Solid Electrolytes. *J. Electrochem. Soc.* 1973, 120, 1289.
- (6) Chiang, Y. M.; Lavik, E. B.; Kosacki, I.; Tuller, H. L.; Ying, J. Y. Defect and Transport Properties of Nanocrystalline CeO_{2-x} . *Appl. Phys. Lett.* 1996, 69, 185–187.
- (7) Lavik, E. B.; Kosacki, I.; Tuller, H. L.; Chiang, Y. M.; Ying, J. Y. Nonstoichiometry and Electrical Conductivity of Nanocrystalline $\text{CeO}_{(2-x)}$. *J. Electroceram.* 1997, 1, 7–14.
- (8) Saranya, A. M.; Morata, A.; Pla, D.; Burriel, M.; Chiabrera, F.; Garbayo, I.; Hornés, A.; Kilner, J. A.; Tarancón, A. Unveiling the Outstanding Oxygen Mass Transport Properties of Mn-Rich Perovskites in Grain Boundary-Dominated $\text{La}_{0.8}\text{Sr}_{0.2}(\text{Mn}_{1-x}\text{Co}_x)_{0.85}\text{O}_{3\pm\Delta}$ Nanostructures. *Chem. Mater.* 2018, 30, 5621–5629.
- (9) Navickas, E.; Huber, T. M.; Chen, Y.; Hetaba, W.; Holzlechner, G.; Rupp, G.; Stöger-Pollach, M.; Friedbacher, G.; Hutter, H.; Yildiz, B.; Fleig, J. Fast Oxygen Exchange and Diffusion Kinetics of Grain Boundaries in Sr-Doped LaMnO_3 Thin Films. *Phys. Chem. Chem. Phys.* 2015, 17, 7659–7669.
- (10) Balaya, P.; Jamnik, J.; Fleig, J.; Maier, J. Mesoscopic Electrical Conduction in Nanocrystalline SrTiO_3 . *Appl. Phys. Lett.* 2006, 88, 062109.
- (11) Ohtomo, A.; Hwang, H. Y. A High-Mobility Electron Gas at the $\text{LaAlO}_3/\text{SrTiO}_3$ Heterointerface. *Nature* 2004, 427, 423–426.
- (12) Thiel, S.; Hammerl, G.; Schmehl, A.; Schneider, C. W.; Mannhart, J. Tunable Quasi-Two-Dimensional Electron Gases in Oxide Heterostructures. *Science* 2006, 313, 1942–1945.
- (13) Chen, T.; Harrington, G. F.; Matsuda, J.; Sasaki, K.; Pham, D.; Corral, E. L.; Perry, N. H. Modifying Grain Boundary Ionic/Electronic Transport in Nano-Sr- and Mg- Doped $\text{LaGaO}_{3-\delta}$ by Sintering Variations. *J. Electrochem. Soc.* 2019, 166, F569–F580.
- (14) Park, H. J.; Kwak, C.; Lee, S. M. Mixed Conduction Behavior in Nanostructured Lanthanum Gallate. *Electrochem. Commun.* 2009, 11, 962–964.
- (15) Maier, J. Nanoionics: Ion Transport and Electrochemical Storage in Confined Systems. *Nat. Mater.* 2005, 4, 805–815.
- (16) Chiabrera, F.; Garbayo, I.; López-Conesa, L.; Martín, G.; Ruiz-Caridad, A.; Walls, M.; Ruiz-González, L.; Kordatos, A.; Núñez, M.;

Morata, A.; Estradé, S.; Chroneos, A.; Peiró, F.; Tarancón, A. Engineering Transport in Manganites by Tuning Local Non-stoichiometry in Grain Boundaries. *Adv. Mater.* **2019**, *31*, 1805360.

(17) Guo, X. Peculiar Size Effect in Nanocrystalline BaTiO_3 . *Acta Mater.* **2013**, *61*, 1748–1756.

(18) Kim, S.; Fleig, J.; Maier, J. Space Charge Conduction: Simple Analytical Solutions for Ionic and Mixed Conductors and Application to Nanocrystalline Ceria. *Phys. Chem. Chem. Phys.* **2003**, *5*, 2268–2273.

(19) Sun, L.; Marrocchelli, D.; Yildiz, B. Edge Dislocation Slows Down Oxide Ion Diffusion in Doped CeO_2 by Segregation of Charged Defects. *Nat. Commun.* **2015**, *6*, 6294.

(20) Marrocchelli, D.; Sun, L.; Yildiz, B. Dislocations in SrTiO_3 : Easy to Reduce but Not So Fast for Oxygen Transport. *J. Am. Chem. Soc.* **2015**, *137*, 4735–4748.

(21) Porz, L.; Fromling, T.; Nakamura, A.; Li, N.; Maruyama, R.; Matsunaga, K.; Gao, P.; Simons, H.; Dietz, C.; Rohnke, M.; Janek, J.; Rodel, J. Conceptual Framework for Dislocation-Modified Conductivity in Oxide Ceramics Deconvoluting Mesoscopic Structure, Core, and Space Charge Exemplified for SrTiO_3 . *ACS Nano* **2020**, DOI: 10.1021/acsnano.0c04491.

(22) Furushima, Y.; Nakamura, A.; Tochigi, E.; Ikuhara, Y.; Toyoura, K.; Matsunaga, K. <1010> Dislocation at a {2110} Low-Angle Grain Boundary in LiNbO_3 . *J. Mater. Sci.* **2018**, *53*, 333–344.

(23) Korte, C.; Keppner, J.; Peters, A.; Schichtel, N.; Aydin, H.; Janek, J. Coherency Strain and Its Effect on Ionic Conductivity and Diffusion in Solid Electrolytes—An Improved Model for Nanocrystalline Thin Films and a Review of Experimental Data. *Phys. Chem. Chem. Phys.* **2014**, *16*, 24575–24591.

(24) Garbayo, I.; Baiutti, F.; Morata, A.; Tarancón, A. Engineering Mass Transport Properties in Oxide Ionic and Mixed Ionic-Electronic Thin Film Ceramic Conductors for Energy Applications. *J. Eur. Ceram. Soc.* **2019**, *39*, 101–114.

(25) Navickas, E.; Chen, Y.; Lu, Q.; Wallisch, W.; Huber, T. M.; Bernardi, J.; Stöger-Pollach, M.; Friedbacher, G.; Hutter, H.; Yildiz, B.; Fleig, J. Dislocations Accelerate Oxygen Ion Diffusion in $\text{La}_{0.8}\text{Sr}_{0.2}\text{MnO}_3$ Epitaxial Thin Films. *ACS Nano* **2017**, *11*, 11475–11487.

(26) Szot, K.; Rodenbürger, C.; Bihlmayer, G.; Speier, W.; Ishikawa, R.; Shibata, N.; Ikuhara, Y. Influence of Dislocations in Transition Metal Oxides on Selected Physical and Chemical Properties. *Crystals* **2018**, *8*, 241.

(27) Amodeo, J.; Merkel, S.; Tomas, C.; Carrez, P.; Korte-Kerzel, S.; Cordier, P.; Chevalier, J. Dislocations and Plastic Deformation in MgO Crystals: A Review. *Crystals* **2018**, *8*, 240.

(28) Hirel, P.; Carrez, P.; Cordier, P. From Glissile to Sessile: Effect of Temperature on <110> Dislocations in Perovskite Materials. *Scr. Mater.* **2016**, *120*, 67–70.

(29) Fan, Y.; Osetskiy, Y. N.; Yip, S.; Yildiz, B. Mapping Strain Rate Dependence of Dislocation-Defect Interactions by Atomistic Simulations. *Proc. Natl. Acad. Sci. U. S. A.* **2013**, *110*, 17756.

(30) Gilardi, E.; Gregori, G.; Wang, Y.; Sigle, W.; van Aken, P. A.; Maier, J. Interface Effects on the Ion Transport of Epitaxial $\text{Y}_2\text{Zr}_2\text{O}_7$ Films. *ACS Appl. Mater. Interfaces* **2017**, *9*, 27257–27265.

(31) Liu, X.-Y.; Martinez, E.; Uberuaga, B. P. Dissociated Vacancies and Screw Dislocations in MgO and UO_2 : Atomistic Modeling and Linear Elasticity Analysis. *Sci. Rep.* **2019**, *9*, 6499.

(32) Spurgeon, S. R.; Sushko, P. V.; Devaraj, A.; Du, Y.; Droubay, T.; Chambers, S. A. Multimodal Imaging of Cation Disorder and Oxygen Deficiency-Mediated Phase Separation in Double Perovskite Oxides. *Microsc. Microanal.* **2017**, *23*, 1678–1679.

(33) Du, H.; Jia, C.-L.; Houben, L.; Metlenko, V.; De Souza, R. A.; Waser, R.; Mayer, J. Atomic Structure and Chemistry of Dislocation Cores at Low-Angle Tilt Grain Boundary in SrTiO_3 Bicrystals. *Acta Mater.* **2015**, *89*, 344–351.

(34) Feng, B.; Ishikawa, R.; Kumamoto, A.; Shibata, N.; Ikuhara, Y. Atomic Scale Origin of Enhanced Ionic Conductivity at Crystal Defects. *Nano Lett.* **2019**, *19*, 2162–2168.

(35) Rodenbürger, C.; Menzel, S.; Wrana, D.; Gensch, T.; Korte, C.; Krok, F.; Szot, K. Current Channeling Along Extended Defects During Electroreduction of SrTiO_3 . *Sci. Rep.* **2019**, *9*, 2502.

(36) Yang, S.; Xiong, L.; Deng, Q.; Chen, Y. Concurrent Atomistic and Continuum Simulation of Strontium Titanate. *Acta Mater.* **2013**, *61*, 89–102.

(37) Atkinson, A. Surface and Interface Mass Transport in Ionic Materials. *Solid State Ionics* **1988**, *28–30*, 1377–1387.

(38) Chadwick, A. V. Transport in Defective Ionic Materials: From Bulk to Nanocrystals. *Phys. Status Solidi A* **2007**, *204*, 631–641.

(39) Adeppali, K. K.; Kelsch, M.; Merkle, R.; Maier, J. Influence of Line Defects on the Electrical Properties of Single Crystal TiO_2 . *Adv. Funct. Mater.* **2013**, *23*, 1798–1806.

(40) Miller, E. J.; Schaadt, D. M.; Yu, E. T.; Poblenz, C.; Elsass, C.; Speck, J. S. Reduction of Reverse-Bias Leakage Current in Schottky Diodes on Gan Grown by Molecular-Beam Epitaxy Using Surface Modification with an Atomic Force Microscope. *J. Appl. Phys.* **2002**, *91*, 9821–9826.

(41) Zhao, C. W.; Xing, Y. M.; Zhou, C. E.; Bai, P. C. Experimental Examination of Displacement and Strain Fields in an Edge Dislocation Core. *Acta Mater.* **2008**, *56*, 2570–2575.

(42) Prakash, A.; Guénolé, J.; Wang, J.; Müller, J.; Spiecker, E.; Mills, M. J.; Povstugar, I.; Choi, P.; Raabe, D.; Bitzek, E. Atom Probe Informed Simulations of Dislocation-Precipitate Interactions Reveal the Importance of Local Interface Curvature. *Acta Mater.* **2015**, *92*, 33–45.

(43) Otsuka, K.; Kuwabara, A.; Nakamura, A.; Yamamoto, T.; Matsunaga, K.; Ikuhara, Y. Dislocation-Enhanced Ionic Conductivity of Yttria-Stabilized Zirconia. *Appl. Phys. Lett.* **2003**, *82*, 877–879.

(44) Otsuka, K.; Matsunaga, K.; Nakamura, A.; Ii, S.; Kuwabara, A.; Yamamoto, T.; Ikuhara, Y. Effects of Dislocations on the Oxygen Ionic Conduction in Yttria Stabilized Zirconia. *Mater. Trans.* **2004**, *45*, 2042–2047.

(45) Sillassen, M.; Eklund, P.; Pryds, N.; Johnson, E.; Helmersson, U.; Böttiger, J. Low-Temperature Superionic Conductivity in Strained Yttria-Stabilized Zirconia. *Adv. Funct. Mater.* **2010**, *20*, 2071–2076.

(46) Yeh, T.-H.; Lin, R.-D.; Cherng, J.-S. Effects of Residual Stress and Interface Dislocations on the Ionic Conductivity of Yttria Stabilized Zirconia Nano-Films. *Thin Solid Films* **2015**, *574*, 66–70.

(47) Harrington, G. F.; Cavallaro, A.; McComb, D. W.; Skinner, S. J.; Kilner, J. A. The Effects of Lattice Strain, Dislocations, and Microstructure on the Transport Properties of Ysz Films. *Phys. Chem. Chem. Phys.* **2017**, *19*, 14319–14336.

(48) Schichtel, N.; Korte, C.; Hesse, D.; Janek, J. Elastic Strain at Interfaces and Its Influence on Ionic Conductivity in Nanoscaled Solid Electrolyte Thin Films—Theoretical Considerations and Experimental Studies. *Phys. Chem. Chem. Phys.* **2009**, *11*, 3043.

(49) Schichtel, N.; Korte, C.; Hesse, D.; Zakharov, N.; Butz, B.; Gerthsen, D.; Janek, J. On the Influence of Strain on Ion Transport: Microstructure and Ionic Conductivity of Nanoscale $\text{YSZ}|\text{Sc}_2\text{O}_3$ Multilayers. *Phys. Chem. Chem. Phys.* **2010**, *12*, 14596.

(50) Adeppali, K. K.; Kelsch, M.; Merkle, R.; Maier, J. Enhanced Ionic Conductivity in Polycrystalline TiO_2 by “One-Dimensional Doping. *Phys. Chem. Chem. Phys.* **2014**, *16*, 4942–4951.

(51) Adeppali, K. K.; Yang, J.; Maier, J.; Tuller, H. L.; Yildiz, B. Tunable Oxygen Diffusion and Electronic Conduction in SrTiO_3 by Dislocation-Induced Space Charge Fields. *Adv. Funct. Mater.* **2017**, *27*, 1700243.

(52) Schraknepper, H.; Weirich, T. E.; De Souza, R. A. The Blocking Effect of Surface Dislocations on Oxygen Tracer Diffusion in SrTiO_3 . *Phys. Chem. Chem. Phys.* **2018**, *20*, 15455–15463.

(53) Liu, Z.; Zarotti, F.; Shi, Y.; Yang, N. Dislocations Promoted a-Site Nonstoichiometry and Their Impacts on the Proton Transport Properties of Epitaxial Barium Zirconate Thin Films. *J. Phys. Chem. C* **2019**, *123*, 20698–20704.

(54) Felici, R.; Aruta, C.; Yang, N.; Zarotti, F.; Foglietti, V.; Cantoni, C.; Tebano, A.; Carlà, F.; Balestrino, G. Regular Network of Misfit Dislocations at the $\text{BaZr}_{0.8}\text{Y}_{0.2}\text{O}_{3-x}|\text{NdGaO}_3$ Interface and Its Role in Proton Conductivity. *Phys. Status Solidi B* **2019**, *256*, 1800217.

(55) Li, X.; Zhang, L.; Tang, Z.; Liu, M. Fast Oxygen Transport in Bottleneck Channels for Y-Doped BaZrO_3 : A Reactive Molecular Dynamics Investigation. *J. Phys. Chem. C* **2019**, *123*, 25611–25617.

(56) Korte, C.; Schichtel, N.; Hesse, D.; Janek, J. Influence of Interface Structure on Mass Transport in Phase Boundaries between Different Ionic Materials. *Monatsh. Chem.* **2009**, *140*, 1069–1080.

(57) Rodenbucher, C.; Bittkau, K.; Bihlmayer, G.; Wrana, D.; Gensch, T.; Korte, C.; Krok, F.; Szot, K. Mapping the Conducting Channels Formed Along Extended Defects in SrTiO_3 by Means of Scanning Near-Field Optical Microscopy. *Sci. Rep.* **2020**, *10*, 17763.

(58) Zhang, F.; Walker, A. M.; Wright, K.; Gale, J. D. Defects and Dislocations in MgO : Atomic Scale Models of Impurity Segregation and Fast Pipe Diffusion. *J. Mater. Chem.* **2010**, *20*, 10445–10451.

(59) Chen, C.-C.; Zhu, C.; White, E. R.; Chiu, C.-Y.; Scott, M. C.; Regan, B. C.; Marks, L. D.; Huang, Y.; Miao, J. Three-Dimensional Imaging of Dislocations in a Nanoparticle at Atomic Resolution. *Nature* **2013**, *496*, 74–77.

(60) Miller, M. K. Atom Probe Tomography Characterization of Solute Segregation to Dislocations and Interfaces. *J. Mater. Sci.* **2006**, *41*, 7808–7813.

(61) Xu, X.; Carr, C.; Chen, X.; Myers, B. D.; Huang, R.; Yuan, W.; Choi, S.; Yi, D.; Phatak, C.; Haile, S. M. Local Multimodal Electro-Chemical-Structural Characterization of Solid-Electrolyte Grain Boundaries. *Adv. Energy Mater.* **2021**, *11*, 2003309.

(62) Xu, X.; Liu, Y.; Wang, J.; Isheim, D.; Dravid, V. P.; Phatak, C.; Haile, S. M. Variability and Origins of Grain Boundary Electric Potential Detected by Electron Holography and Atom-Probe Tomography. *Nat. Mater.* **2020**, *19*, 887–893.

(63) Zhang, Z.; Sigle, W.; De Souza, R. A.; Kurtz, W.; Maier, J.; Rühle, M. Comparative Studies of Microstructure and Impedance of Small-Angle Symmetrical and Asymmetrical Grain Boundaries in SrTiO_3 . *Acta Mater.* **2005**, *53*, 5007–5015.

(64) McLachlan, D. S.; Blaszkiewicz, M.; Newnham, R. E. Electrical Resistivity of Composites. *J. Am. Ceram. Soc.* **1990**, *73*, 2187–2203.

(65) Kidner, N. J.; Perry, N. H.; Mason, T. O.; Garboczi, E. J. The Brick Layer Model Revisited: Introducing the Nano-Grain Composite Model. *J. Am. Ceram. Soc.* **2008**, *91*, 1733–1746.

(66) Perry, N. H.; Kim, S.; Mason, T. O. Local Electrical and Dielectric Properties of Nanocrystalline Yttria-Stabilized Zirconia. *J. Mater. Sci.* **2008**, *43*, 4684–4692.

(67) Mebane, D. S.; De Souza, R. A. A Generalised Space-Charge Theory for Extended Defects in Oxygen-Ion Conducting Electrolytes: From Dilute to Concentrated Solid Solutions. *Energy Environ. Sci.* **2015**, *8*, 2935–2940.

(68) Harrington, G. F.; Sun, L.; Yildiz, B.; Sasaki, K.; Perry, N. H.; Tuller, H. L. The Interplay and Impact of Strain and Defect Association on the Conductivity of Rare-Earth Substituted Ceria. *Acta Mater.* **2019**, *166*, 447–458.

(69) Yildiz, B. “Stretching” the Energy Landscape of Oxides—Effects on Electrocatalysis and Diffusion. *MRS Bull.* **2014**, *39*, 147–156.

(70) Lin, Y.-Y.; Yong, A. X. B.; Gustafson, W. J.; Reedy, C. N.; Ertekin, E.; Krogstad, J. A.; Perry, N. H. Toward Design of Cation Transport in Solid-State Battery Electrolytes: Structure-Dynamics Relationships. *Curr. Opin. Solid State Mater. Sci.* **2020**, *24*, 100875.

(71) Szot, K.; Speier, W.; Bihlmayer, G.; Waser, R. Switching the Electrical Resistance of Individual Dislocations in Single-Crystalline SrTiO_3 . *Nat. Mater.* **2006**, *5*, 312–320.

(72) Clarke, D. R. The Microstructural Location of the Intergranular Metal-Oxide Phase in a Zinc Oxide Varistor. *J. Appl. Phys.* **1978**, *49*, 2407–2411.

(73) Fang, T.-T.; Shiao, H.-K. Mechanism for Developing the Boundary Barrier Layers of $\text{CaCu}_3\text{Ti}_4\text{O}_{12}$. *J. Am. Ceram. Soc.* **2004**, *87*, 2072–2079.

(74) Sun, L.; Yildiz, B. Stabilizing Single Atoms and a Lower Oxidation State of Cu by a 1/2 [110]{100} Edge Dislocation in CuCeO_2 . *Phys. Rev. Mater.* **2019**, *3*, 025801.

(75) Butler, K. T.; Davies, D. W.; Cartwright, H.; Isayev, O.; Walsh, A. Machine Learning for Molecular and Materials Science. *Nature* **2018**, *559*, 547–555.

(76) Kondo, S.; Shibata, N.; Mitsuma, T.; Tochigi, E.; Ikuhara, Y. Dynamic Observations of Dislocation Behavior in SrTiO_3 by in Situ Nanoindentation in a Transmission Electron Microscope. *Appl. Phys. Lett.* **2012**, *100*, 181906.

(77) Korte, C.; Peters, A.; Janek, J.; Hesse, D.; Zakharov, N. Ionic Conductivity and Activation Energy for Oxygen Ion Transport in Superlattices—The Semicoherent Multilayer System $\text{Ysz}(\text{ZrO}_2 + 9.5 \text{ mol\% Y}_2\text{O}_3)/\text{Y}_2\text{O}_3$. *Phys. Chem. Chem. Phys.* **2008**, *10*, 4623–4635.

(78) Sandiumenge, F.; Bagués, N.; Santiso, J.; Paradinas, M.; Pomar, A.; Konstantinovic, Z.; Ocal, C.; Balcells, L.; Casanove, M.-J.; Martínez, B. Misfit Dislocation Guided Topographic and Conduction Patterning in Complex Oxide Epitaxial Thin Films. *Adv. Mater. Interfaces* **2016**, *3*, 1600106.